cerebral blood volume (CBV) to the kinetic $^{15}O_2$ data obtained from a single PET scan after the bolus administration of $^{15}O_2$. To minimize errors which result from neglecting RW, only the initial 3 mins of data after the bolus inhalation of $^{15}O_2$ were used when calculating the parameters. This approach has been applied to evaluate the magnitude of increase in $CMRO_2$ relative to that in CBF during cognitive stimulation tasks (Fujita *et al*, 1999; Vafaee and Gjedde, 2000; Okazawa *et al*, 2001*a*, *b*; Yamauchi *et al*, 2003; Mintun *et al*, 2002), but one of the drawbacks to this technique is the lack of accurate statistics, which is due to the use of a short scan duration.

Iida *et al* (1993) have developed a mathematical formula to predict the production of RW based on a physiologic model, which allows prolongation of the PET acquisition period with an additional statistical accuracy. The formula assumes a fixed rate constant for production of RW from $^{15}O_2$ in the body. This is based on the fact that the observed rate constant did not vary among clinical subjects, and thus causes nonsignificant errors in $CMRO_2$. However, the study is limited only to human subjects studied at rest, and results have not been verified using other species such as rat and mouse (Magata *et al*, 2003; Temma *et al*, 2006; Yee *et al*, 2006). Also, the findings have not been evaluated on humans who are under physiologic stress, though under such conditions the whole-body oxygen consumption is expected to change. Moreover, it is important to extend the approach to physiologically stressed conditions as recent progress for assessing $CMRO_2$ and CBF simultaneously from a short period dynamic scan by using a dual tracer autoradiography (DARG) (Kudomi *et al*, 2005). The DARG has enabled the $^{15}O_2$ PET to assess $CMRO_2$ and CBF simultaneously at various physiologically activated conditions.

The aim of this study is to verify the method used to estimate the arterial RW during the $^{15}O_2$ inhalation for simultaneous determination of $CMRO_2$ and CBF from the rapid procedures of $^{15}O_2$ PET. The feasibility of a simplified procedure is also being investigated. Applicability of this approach was tested for a wide range of species under various physiologic conditions. Experiments were designed to apply for different species as well as different physiologic conditions. A simulation study was also performed to evaluate the level of error sensitivity associated with this approach.

Materials and methods

Theory

Variables used in the recirculating water model are summarized in Table 1. The mathematical model that formulates the time-dependent RW in arterial blood consists of three rate constants: (1) the production rate of RW or k (per min), proportional to oxidative metabolism in the total body system ($BMRO_2$), (2) the forward diffusion rate (k_w, per min) of the metabolized ^{15}O-water between the blood and interstitial spaces in the body, and (3) the backward diffusion rate (k_2, per min) of the metabolized ^{15}O-water between the blood and interstitial spaces in the body. The differential equations for the arterial activity concentration of ^{15}O-water at a time t (secs) ($A_w(t)$, Bq/mL), after the physical decay correction can be expressed as follows (Huang *et al*, 1991):

$$\frac{d}{dt}A_w(t) = k \cdot A_o(t) - k_w \cdot A_w(t) + k_2 \cdot C(t) \quad (1a)$$

$$\frac{d}{dt}C(t) = k_w \cdot A_w(t) - k_2 \cdot C(t) \quad (1b)$$

$$A_t(t) = A_o(t) + A_w(t) \quad (1c)$$

where $A_o(t)$ and $A_t(t)$ denote the radioactivity concentration of the arterial $^{15}O_2$ and the total radioactivity from both

Table 1 Variables used in the recirculating water model

Symbol	*Description*	*Unit*
A_o	Radioactivity concentration of arterial $^{15}O_2$	Bq/mL
A_w	Radioactivity concentration of arterial $H_2^{15}O$	Bq/mL
A_t	Total radioactivity concentration from arterial $^{15}O_2$ and $H_2^{15}O$	Bq/mL
A_{plasma}	Radioactivity concentration of arterial plasma	Bq/mL
C	Activity concentration of $H_2^{15}O$ in peripheral tissue in a body	Bq/mL
Fi_{O_2}	Oxygen concentration in inhaled gas	%
Fe_{O_2}	Oxygen concentration in expired gas	%
k	Production rate of recirculating $H_2^{15}O$	per min
k_{BM}	Production rate of recirculating $H_2^{15}O$ obtained from BM approach	per min
k_w	Forward diffusion rate of $H_2^{15}O$ from blood to body interstitial space	per min
k_2	Backward diffusion rate of $H_2^{15}O$ from blood to body interstitial space	per min
λ	Decay constant of ^{15}O (= 0.00567 per sec)	per sec
v	Stroke volume	mL
p	k_w/k_2	
r	Respiration rate	per min
R	Fractional water content ratio in whole blood to that in the plasma	
R_{O_2}	Rate of oxidative metabolism in the whole-body system	mL/min
Δt	Delayed appearance time of recirculating water	secs
V_{O_2}	Total volume of molecular oxygen in total blood	mL
V_{TB}	Total volume of blood in a body	mL

$^{15}O_2$ and $H_2^{15}O$, respectively. $C(t)$ is an activity concentration of $H_2^{15}O$ in the peripheral tissue of the total body. Assuming a delayed appearance of RW by Δt (Iida *et al*, 1993), the following equation can be obtained:

$$A_w(t+\Delta t) = k(\alpha_1 \cdot A_t(t) \otimes \exp(-\beta_1 t) + \alpha_2 \cdot A_t(t) \otimes \exp(-\beta_2 t)) \quad (2)$$

where $\otimes$ denotes the convolution integral and:

$$\alpha_{1,2} = \frac{a - 2c \pm \sqrt{a^2 - 4b}}{\pm 2\sqrt{a^2 - 4b}}, \quad \beta_{1,2} = \frac{a \pm \sqrt{a^2 - 4b}}{2},$$
$$a = k + k_w + k_w/p, \quad b = k \cdot k_w/p, \quad c = k_w/p, \quad p = k_w/k_2 \quad (3)$$

Following four approaches were performed to determine the rate constants and $A_w(t)$.

Approach by four parameters fitting: Four parameters, k, Δt, k_w, and p ($=k_w/k_2$), can be determined from the observed RW ($A_w(t)$) and the $A_t(t)$ curves by means of the nonlinear least square fitting (4PF approach).

Approach by one parameter fitting: Once three parameters, Δt, k_w, and p, are fixed by averaging values determined by the 4PF approach, k can then be determined by fitting the Equation 2 to measured $A_w(t)$ from $A_t(t)$ (1PF approach). In this procedure, single datum is sufficient, and thus k can be determined from $A_t(t)$ and the RW counts sampled at a single time point.

Approach from steady-state condition: Similarly to the 1PF procedures, k can be determined from the steady state condition, which is achieved by a continuous administration of $^{15}O_2$ as follows (SS approach). Incorporating the decay constant of ^{15}O ($\lambda = 0.00567$ per secs) into Equations 1a and 1b provides:

$$\frac{d}{dt}A^*_w(t) = k \cdot A^*_o(t) - k_w \cdot A^*_w(t) + k_2 \cdot C^*(t) - \lambda \cdot A^*_w(t) \quad (4a)$$

$$\frac{d}{dt}C^*(t) = k_w \cdot A^*_w(t) - k_2 \cdot C^*(t) - \lambda \cdot C^*(t) \quad (4b)$$

where variables with the symbol * denote that no correction was made for the radioactivity decay of ^{15}O. After continuously administrating $^{15}O_2$, the radioactivity distribution of $A^*_o(t)$, $A^*_w(t)$, and $C^*_t(t)$ reaches a steady state. Thus, the following equations hold:

$$0 = k \cdot A^*_o(t) - k_w A^*_w(t) + k_2 C^*(t) - \lambda A^*_w(t) \quad (5a)$$

$$0 = k_w A^*_w(t) - k_2 C^*(t) - \lambda C^*(t) \quad (5b)$$

Given the values of k_w and k_2 which are determined as averages of 4PF, k can be calculated from the arterial $^{15}O_2$ and $H_2^{15}O$ concentrations at steady state as follows:

$$k = \lambda\left(\frac{k_w + k_2 + \lambda}{k_2 + \lambda}\right)\frac{A^*_w(t)}{A^*_o(t)} \quad (6)$$

Approach by the rate of whole body oxidative metabolism: In this study, an alternative approach is provided to obtain k, from the rate of oxidative metabolism in the whole-body system (BM approach). With this alternative approach, we assume that the production rate of RW or k is proportional to the rate of oxidative metabolism in the whole-body system (i.e., $BMRO_2$ (R_{O_2}, mL/min)). The rate of oxidative metabolism may change dependent on physiologic status of the subject. In addition, we assumed that this index can be defined from the difference of oxygen concentration between inhaled and exhaled trachea air samples. Therefore, the above can be expressed as follows:

$$k = c \cdot \frac{R_{O_2}}{V_{O_2}} \text{ (per min)} \quad (7a)$$

or

$$k_{BM} = \frac{k}{c} = \frac{R_{O_2}}{1.36 \cdot Hb \cdot V_{TB}} \quad (7b)$$

where c is the proportionality constant, k_{BM} the production rate of RW obtained from BM approach, V_{O_2} (mL) the total volume of molecular oxygen in total blood, 1.36 mL/g the amount of oxygen molecules combined with unit mass of hemoglobin, Hb (g/mL) represents the hemoglobin concentration in the arterial blood, and V_{TB} (mL) is the total volume of blood in the body.

Simulation

A series of simulation studies were performed to investigate the effects of errors on estimated $CMRO_2$ value in the model parameters (k, Δt, k_w, and p). In these simulations, a typical arterial blood time activity curve (TAC) of $^{15}O_2$ and $H_2^{15}O$ after DARG protocol (Kudomi *et al*, 2005) obtained in a monkey study was used. RW TACs were generated from the whole blood TAC by assuming baseline values of k as 0.13, 0.11, 0.34, and 0.73 per min, Δt as 20, 11, 5, and 3 secs, k_w as 0.38, 0.43, 0.98, and 0.87 per min, and p as 1.31, 1.01, 0.98, and 0.83, corresponding to humans, pigs, monkeys, and rats, respectively. Tissue TACs were generated by assuming CBF = 50 mL/min per 100 g and OEF = 0.4 ($CMRO_2$ was defined as: $CMRO_2 = CBF \times OEF \times C_aO_2$, where C_aO_2 is the arterial oxygen content. This simulation was intended to investigate magnitude of error as a percentage difference, so that arbitrary value of C_aO_2 was assumed) (Hayashi *et al*, 2003), using a kinetic formula for oxygen and water in the brain tissue (Mintun *et al*, 1984; Shidahara *et al*, 2002; Kudomi *et al*, 2005). $CMRO_2$ values were calculated by the DARG method (Kudomi *et al*, 2005), in which RW TACs were separated from the whole blood by changing k from 0.0 to 1.0 per min, Δt from 0 to 30 secs, k_w from 0.0 to 2.0 per min, and p from 0.0 to 2.0, respectively. Errors in the estimated $CMRO_2$ were presented as a percentage difference from the assumed true values.

Subjects

Subjects consisted of four groups including monkeys, pigs, rats, and clinical patients. Monkeys were six healthy *macaca fascicularis* with body weight of 5.2 ± 0.8 kg and age ranging from 3- to 4-year old. Pigs were three farm pigs

with body weight of 38 ± 9 kg and age from 4 to 12 months. Rats were 12 male Wistar rats with body weight of 300 ± 54 g and age from 7 to 8 weeks. All animals were studied during anesthesia. The animals were maintained and handled in accordance with guidelines for animal research on Human Care and Use of Laboratory Animals (Rockville, National Institute of Health/Office for Protection from Research Risks, 1996). The study protocol was approved by the Subcommittee for Laboratory Animal Welfare of National Cardiovascular Center.

Human data were retrospectively sampled from an existing database at National Cardiovascular Center which documented subjects who underwent PET examination after the ^{15}O-steady-state protocol. There were 231 total samples, with body weight and age ranging from 58 ± 10 kg, and 63 ± 14 years, respectively. Only the arterial $^{15}O_2$ and $H_2^{15}O$ radioactivity concentrations measured at the steady-state condition were used for the present analysis.

Experimental Protocol

The six monkeys were anesthetized using propofol (4 mg/kg/h) and vecuronium (0.05 mg/kg/h) assigned as a baseline in contrast to the after physiologically stimulated conditions. Animals were intubated and their respiration was controlled by an anesthetic ventilator (Cato, Drager, Germany). Each monkey inhaled 2,200 MBq $^{15}O_2$ for 20 secs. After 3 mins, the monkeys were injected with 370 MBq $H_2^{15}O$ for 30 secs by the anterior tibial vein. This was aimed at assessing both CBF and $CMRO_2$ according to the DARG technique (Kudomi *et al*, 2005). At 30 secs before inhaling $^{15}O_2$ to the monkeys, arterial blood was withdrawn from the femoral artery for 420 secs at a rate of 0.45 mL/min using a Harvard pump (Harvard Apparatus, Holliston, MA, USA). The whole blood TAC was measured with a continuous monitoring system (Kudomi *et al*, 2003) and the $A_t(t)$ was obtained. Meanwhile, we also manually obtained 0.5 mL of arterial blood samples from the contralateral femoral artery at 30, 50, 70, 90, 110, 130, 160, 190, and 360 secs after the $^{15}O_2$ inhalation. For the analysis of sampled blood, 0.2 mL of the blood were used for measurement of the radioactivity concentration of the whole blood, and the rest of the blood sampled (~0.3 mL) was immediately centrifuged for separation to measure the plasma radioactivity concentration ($A_{plasma}(t)$, Bq/mL). The radioactivity concentration was measured using a well counter (Molecular Imaging Laboratory Co. Ltd, Suita, Japan).

In two monkeys, anesthetic level was changed by altering the injection dose of propofol from 4 (baseline) to 8 and then to 12 and 16 mg/kg/h in one monkey, and to 5 and then to 7, 10, and 15 mg/kg/h in the other. In another monkey, $PaCO_2$ level was varied from 39 (baseline) to 47, and then to 33, 26, and 42 mm Hg by changing the respiratory rate. Each measurement for $^{15}O_2$ inhalation and $H_2^{15}O$ injection was initiated after at least 30 mins of applying the physiologic stimulation to achieve a steady state. All procedures were the same as those for the baseline, with the exception of the manual blood sample, which was obtained only once at 70 secs.

Before and after 6 mins of the $^{15}O_2$ inhalation, oxygen concentration in both inhaled (Fi_{O_2}, %) and end-tidal expiratory gas (Fe_{O_2}, %) was measured by the anesthetic ventilator in five out of the six monkeys. Using the respiration rate (r, per min) and the stroke volume (v, mL) indicated on the ventilator, the $BMRO_2$ (R_{O_2} mL/min) was calculated using the following equation:

$$R_{O_2} = (Fi_{O_2} - Fe_{O_2}) \cdot v \cdot r.$$

All monkeys received a PET measurement to assess the $CMRO_2$ at physiologically baseline condition. The scan protocol followed the DARG technique (Kudomi *et al*, 2005) in which a 6-mins single dynamic PET scan was performed in conjunction with the administration of dual tracers (i.e., $^{15}O_2$ followed by $H_2^{15}O$ after a 3-mins interval). PET scanner used was ECAT HR (Siemens-CTI, Knoxville, TN, USA), which provided 47 tomographic slice images for an axial field-of-view of approximately 150 mm. We performed arterial–sinus blood sampling to obtain a global OEF (OEF_{A-V}) (A–V difference approach). We sampled 0.2 mL of arterial and sinus blood simultaneously during each PET scan and measured their oxygen content (C_aO_2 and C_vO_2, respectively) (Kudomi *et al*, 2005). The OEF_{A-V} was calculated as: $OEF_{A-V} = (C_aO_2 - C_vO_2)/C_aO_2$.

With regards to the farm pigs involved in this experiment, we used existing data, which were originally obtained in one of the myocardial projects. During the study, three farm pigs were anesthetized. Anesthesia was induced by ketamine (10 mg/kg) and maintained using propofol (4 mg/kg/h). Animals were intubated and their respiration was controlled by the anesthetic ventilator. Venous blood was labeled with $^{15}O_2$ using a small artificial lung unit (Magata *et al*, 2003). $^{15}O_2$-labeled blood (222 to 700 MBq) was injected for 10 secs via anterior tibial vein. At 30 secs before this injection, arterial blood was withdrawn from the femoral artery at a rate of 0.45 mL/min using the Harvard pump and continued for 420 secs. The whole blood TAC ($A_t(t)$) was then measured with a continuous monitoring system (Kudomi *et al*, 2003). Meanwhile, we manually sampled 0.5 mL of arterial blood from the contralateral femoral artery at 30, 60, 90, 90, 120, 180, 240, and 300 secs after the $^{15}O_2$-labeled blood injection. For the analysis of sampled blood, 0.2 mL of the blood were used for measurement of the radioactivity concentration of the whole blood, and the rest of the blood sampled (~0.3 mL) was immediately centrifuged for separation to measure the plasma radioactivity ($A_{plasma}(t)$, Bq/mL). The radioactivity was measured using the well counter.

Data for rats were also originally obtained for other projects, and only the blood counts were used in this study. Anesthesia was induced with pentobarbital (50 mg/kg). A 10 mL of venous blood was labeled $^{15}O_2$ using a small artificial lung unit as described previously (Magata *et al*, 2003), and approximately 1 mL of $^{15}O_2$-labeled blood (37 to 74 MBq) was injected for 30 secs via the tail vein. Arterial blood samples of 0.1 mL each were obtained from the femoral artery at 5-secs intervals for 60 secs and 10-secs intervals for another 60 secs after the injection. Whole blood radioactivity concentration was measured using the well counter to be used as $A_t(t)$. Arterial blood samples of

0.2 mL each were obtained at 30, 60, 90, and 120 secs, and the plasma radioactivity concentration ($A_{plasma}(t)$) was measured by the well counter.

For clinical patients, the blood radioactivity concentration was obtained from previously performed PET examinations, which followed the steady-state protocol (Hirano *et al*, 1994). Each patient inhaled both $^{15}O_2$ and $C^{15}O_2$ to reach the steady state with an inhalation dose of approximately 1,200 and 500 MBq/min, respectively. Five to seven arterial blood samples were obtained during the steady state from the brachial artery. Mean values of radioactivity concentration of the whole blood and plasma, $A_t(t)$ and $A_{plasma}(t)$, respectively, were obtained for both $^{15}O_2$ and $C^{15}O_2$ PET examination.

Data Analysis

Using the blood activity data obtained from monkeys, pigs, and rats at baseline conditions, k as well as Δt, k_w and p were first determined by the 4PF approach, in which Equation 2 was applied to fit the $A_w(t)$ using the observed $A_t(t)$. Because the solubility of the oxygen is negligibly small in the plasma, we assumed that all radioactivity in plasma fraction comes from $H_2^{15}O$ and that the water content ratio of whole blood to plasma (R) does not change during measurement, which means that the kinetics of water molecules immediately reach equilibrium between the plasma and the cellular fraction (Mintun *et al*, 1984; Iida *et al*, 1993). Thus, $A_w(t)$ was obtained from the equation: $A_w(t) = A_{plasma}(t) \cdot R$, where R value was obtained from the sampled blood at the end of the scan (at which all the radioactivity in the blood can be considered as coming from $H_2^{15}O$ because inhaled $^{15}O_2$ is all metabolized).

Given that the values of Δt, k_w, and p were averages determined from 4PF for monkeys, pigs, and rats, only k was determined by fitting Equation 2 to A_w. This was calculated at various points in time, more specifically, in 30, 50, 70, 90, 110, 130, 160, and 190 secs for monkeys, in 30, 60, 90, 90, 120, 180, and 240 secs for pigs, and in 30, 60, 90, and 120 secs for rats. The optimal time point for k under the 1PF approach was determined, so that $(k_{4PF}-k_{1PF})/k_{4PF}$ reaches a minimal value. Here, k_{4PF} and k_{1PF} denote k values determined by the 4PF and 1PF approaches, respectively. The values of k in monkeys at baseline condition, together with those in pigs and rats were compared between 4PF and 1PF approaches, in which a k value from the optimal single time point was used.

In three of the monkeys, which were physiologically stimulated, k of 1PF approach was obtained using single time point of A_w. Assuming the total blood volume (V_{TB}) for monkeys as 360 mL (Lindstedt and Schaeffer, 2002), and using Hb as measured value in each experiment, k_{BM} was calculated from R_{O_2} according to Equation 7b. Then, k_{BM} obtained as: $k_{BM} = 0.00204R_{O_2}$ was compared with k determined by 1PF.

For clinical data obtained from the steady-state (SS approach) PET examinations, Equation 6 was used to determine the k values of the SS approach for each patient, in which values of k_w and k_2 were 0.38 and 0.29 per min as obtained in a previous work by Huang *et al* (1991).

$CMRO_2$ and OEF values in monkeys at baseline condition were calculated using the RW TACs obtained by four different methods (i.e., directly measured $A_w(t)$ ($n=6$), 4PF ($n=6$), 1PF ($n=6$), and BM approaches ($n=5$)). Regions-of-interest were selected for over the whole brain, and $CMRO_2$ and OEF values were obtained in those regions-of-interest. The $CMRO_2$ values compared among the four methods mentioned above to estimate RW TACs. The Bland–Altman method was applied to analyze the agreement of OEF values between the methods. Also, OEF values were compared with OEF_{A-V}.

All data were presented as mean ± 1 standard deviation. Student's t-test was used and Pearson's regression analysis was applied to compare two variables. A probability value of <0.05 was considered statistically significant.

Results

Figure 1 shows results from the simulation study, and shows the magnitude of errors in $CMRO_2$ calculated by the DARG method as well as errors in the parameters, k, Δt, k_w, and p. Errors in $CMRO_2$ were most sensitive to errors in k amongst all species, namely the production rate constant of RW in the arterial blood. After errors in k, errors in $CMRO_2$ were sensitive to errors in Δt. Errors in k_w and p, however, appeared to cause relatively insignificant errors in $CMRO_2$. More specifically, only 5 to 10% errors are caused in $CMRO_2$ by a change of ± 50% in k_w and p.

Figures 2A–2C show examples of the arterial whole blood curves (A_t) and RW TAC (A_w) observed in typical studies on a monkey, a pig, and a rat, respectively. The RW curves became constant after a period in all species. The rise time or appearance of the RW curves, $A_w(t)$, was significantly delayed compare to that of whole blood curve, $A_t(t)$. $A_w(t)$ curves fitted by 4PF well reproduced the measured RW curves in three species: monkeys, pigs, and rats. Table 2 summarizes values of k, Δt, k_w, and p obtained by the four parameter fitting (4PF approach), at the baseline for monkeys, pigs, and rats, and also k value obtained by the steady-state formula for clinical patients. Those comparisons showed that the k was significantly different among species ($P<0.001$) except between pig and human subjects, and it was significantly lower in smaller animals. Likewise, Δt showed significant differences among the three species ($P<0.001$), and it was also lower in smaller animals.

Table 3 summarizes k and $CMRO_2$ values obtained from a series of PET experiments performed on six monkeys at baseline condition, and for increased anesthesia (in two monkeys), and changed $PaCO_2$ levels (in one monkey). The best agreement of k values between 4PF and 1PF approaches was obtained from the blood sample data taken at 60, 70, and 60 secs in pigs, monkeys, and rats, respectively, and was used in the 1PF approach. With this

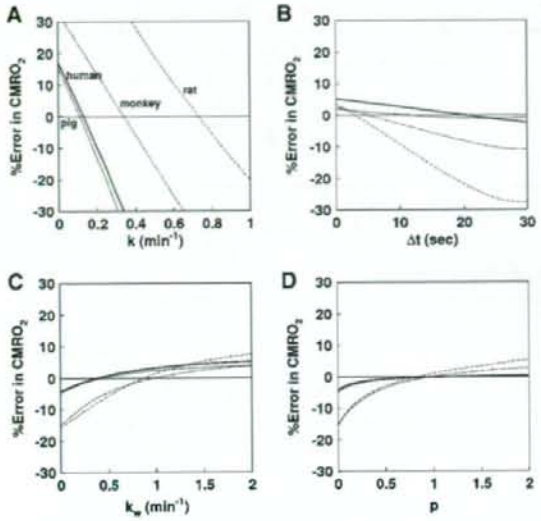

Figure 1 Error in $CMRO_2$ values due to errors in (**A**) k, (**B**) Δt, (**C**) k_w, and (**D**) p for assumed human, pig, monkey and rat. The same type of line indicates the same species. The percentage differences in the $CMRO_2$ values from the assumed true values (Table 1) were plotted as a function of the simulated value of k, Δt, k_w, and p.

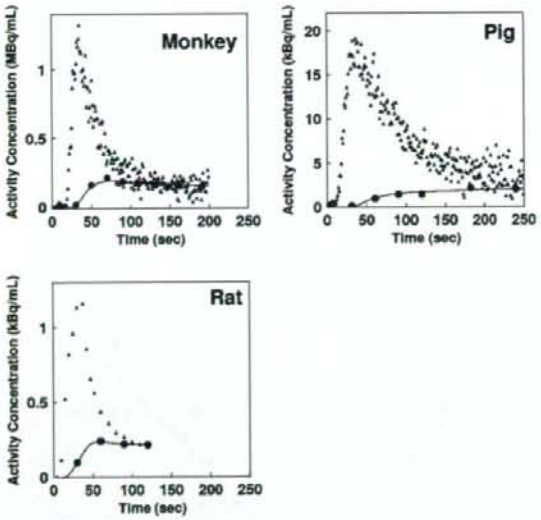

Figure 2 Representative comparison of the measured arterial whole blood and RW time activity curves for monkey, pig, and rat. Closed triangles and closed circles represent the measured whole blood and RW time activity curves, respectively. Estimated time activity curves by 4PF approach were also plotted in a solid line, and indicated a good agreement with the measured one.

optimized calibration protocol, k values were in a good agreement between 4PF and 1PF approaches. As shown in Figure 3, the regression analysis showed significant correlation for 21 animals including 6 monkeys, 3 pigs, and 12 rats ($P<0.001$), and there was no significant difference between the two variables. Figure 4 shows that k values calculated by the 1PF approach (at an optimized time) were in a good agreement with those calculated with the $BMRO_2$. Namely, the regression analysis showed significant correlation ($P<0.001$, $n=16$) and also that there was no significant difference between the two variables. Note that, in the $CMRO_2$ calculation by $BMRO_2$, k values were normalized according to the regression line shown in Figure 4. It should also be noted that calculated $CMRO_2$ values at the baseline shown in Table 3 were not significantly different among the four techniques. The average ($\pm$s.d.) values of obtained OEF were 0.53 ± 0.08, 0.52 ± 0.09, 0.54 ± 0.08, 0.54 ± 0.09, and 0.56 ± 0.04 from A–V difference, directly RW measured approach, 4PF, 1PF, and BM approaches, respectively. The Bland–Altman analysis of OEF values between from A–V difference and from others showed small over/underestimation, that is., with bias $\pm$ s.d. of -0.02 ± 0.09, 0.01 ± 0.07, 0.01 ± 0.08, and 0.02 ± 0.09, by direct RW, 4PF, 1PF, and BM approaches, respectively. Neither of the current methods (direct RW, 4PF, 1PF, and BM) was significantly different from A–V difference approach.

Discussion

Our study showed that the mathematical formula based on the physiologic model that reproduced the time-dependent concentration of RW in the arterial blood after a short-period inhalation of $^{15}O_2$ is indeed adequate. Our approach also simplified the procedures for sequential assessment of RW in $^{15}O_2$ inhalation PET studies, although previous approaches required frequent blood samples and centrifuges of each arterial blood sample. The present approach is an extension of a previous study by Iida *et al* (1993) and Huang *et al* (1991). It is essential if one intends to apply the rapid $^{15}O_2$ PET technique (Kudomi *et al*, 2005) to pharmacologic and physiologic stress studies on a wide range of species. Because the PET acquisition period can be prolonged >3 mins, statistical accuracy can be significantly improved as compared with Ohta *et al* (1992) and other researchers (Fujita *et al*, 1999; Vafaee and Gjedde, 2000; Okazawa *et al*, 2001*a*, *b*; Yamauchi *et al*, 2003; Mintun *et al*, 2002), under which to avoid effects of RW, the data acquisition period was limited only to <3 mins (Meyer *et al*, 1987; Ohta *et al*, 1992).

The present RW formula consists of three rate parameters of the production rate of RW in the arterial blood (k), and the forward and backward diffusion rate constants of RW between the blood and the peripheral tissues. The k was presumed to correspond to the oxygen metabolism in the total body system, $BMRO_2$, and was in fact shown to be

Table 2 Averaged values of k, Δt, k_w, and p for monkeys, pigs, rat, and human subjects under baseline condition

	Weight (kg)	k *(per min)*	*Δt (secs)*	k_w *(per min)*	p
Monkey	5.2 ± 0.8^a	0.34 ± 0.16^a	4.5 ± 1.4^a	0.98 ± 0.48	0.98 ± 0.30
Pig	38 ± 9^a	$0.11 \pm 0.02^{a,b}$	10.8 ± 1.8^a	0.83 ± 0.19	1.01 ± 0.26
Rat	0.30 ± 0.054^a	0.73 ± 0.16^a	2.9 ± 1.7^a	0.87 ± 0.30	0.83 ± 0.32
Human	58 ± 10^a	$0.129 \pm 0.023^{a,b}$	—	—	—

Monkey: $n = 6$; pig: $n = 3$; rat: $n = 12$; and human: $n = 231$. Measured values were obtained by 4PF for monkey, pig, rats, whereas those for human were obtained using data in a steady-state method.

[a]Denotes $P < 0.001$ for other species.

[b]Denotes that the difference was not significant in k between pig and human subjects.

Table 3 Values of k and $CMRO_2$ in the whole brain region for monkeys under physiologically baseline and stimulated conditions

ID	*Condition*	k *(per min)*			*$CMRO_2$ (mL/min per 100 g)*			
		4PF	*1PF*	*$BMRO_2$*	*Reference*	*4PF*	*1PF*	*$BMRO_2$*
1	BL	0.36	0.42	—	3.7	3.7	3.6	—
2	BL	0.62	0.66	1.24	3.0	3.3	3.4	3.4
3	BL	0.32	0.39	0.83	3.0	3.1	3.0	2.9
	(Dose of propofol)							
4	BL	0.21	0.18	0.55	2.0	2.0	2.0	1.8
	8 mg/kg/h	—	0.30	0.69	—	—	—	—
	12 mg/kg/h	—	0.23	0.52	—	—	—	—
	16 mg/kg/h	—	0.16	0.40	—	—	—	—
5	BL	0.12	0.15	0.31	2.1	2.1	2.0	1.8
	5 mg/kg/h	—	0.15	0.32	—	—	—	—
	7 mg/kg/h	—	0.16	0.35	—	—	—	—
	10 mg/kg/h	—	0.18	0.36	—	—	—	—
	15 mg/kg/h	—	0.071	0.29	—	—	—	—
	($PaCO_2$ level)							
6	BL	0.43	0.46	0.95	2.8	3.1	3.0	3.3
	47 mm Hg	—	0.20	0.64	—	—	—	—
	33 mm Hg	—	0.21	0.46	—	—	—	—
	26 mm Hg	—	0.14	0.28	—	—	—	—
	42 mm Hg	—	0.33	0.82	—	—	—	—

4PF, four parameters fitting; 1PF, one parameter fitting; $BMRO_2$, total body metabolic rate of oxygen; BL, baseline condition.
Reference: RW TAC was obtained using measured RW data at a baseline condition in all monkeys ($n = 6$). No statistically significant differences were found in $CMRO_2$ between reference and other techniques.

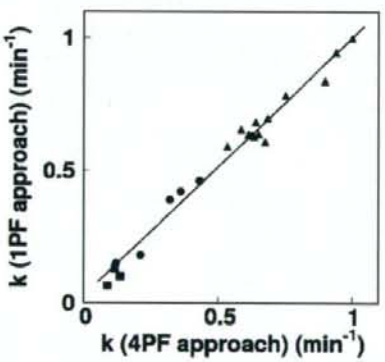

Figure 3 Comparison of the production rates of RW (k, per min) obtained by 4PF and those by 1PF. Squares, circles, and triangles correspond to pigs, monkeys, and rats, respectively. The regression line was $y = 0.97x + 0.026$ (per min) ($r = 0.98$).

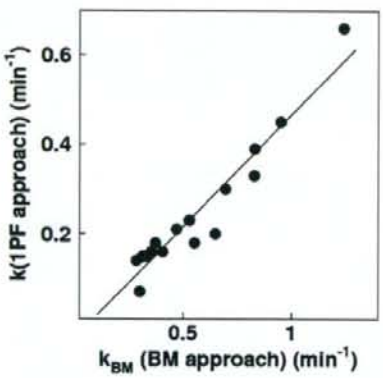

Figure 4 Comparison of the production rates of RW obtained by BM approach and those by 1PF approach in five monkeys at various anesthetic and $PaCO_2$ levels. The regression line was $y = 0.50x - 0.034$ (per min) ($r = 0.95$).

significantly correlated to $BMRO_2$, as measured from the trachea gas sampling (Figure 4). The latter two parameters (k_w and p) appeared to be consistent and did not differ across various species (Table 2). Also, change in those parameters was less sensitive in $CMRO_2$ (Figure 1). These findings suggest that the production of RW after inhalation of $^{15}O_2$ could be described only by a single parameter of k, as shown in Figure 3, although further studies are required to validate this because the method was only tested in a group with small number of subjects of particular physiologic situation (under anesthesia) and has not been applied to different populations. It is also important to note that this parameter (k) estimated from the $BMRO_2$ (i.e., BM approach) provided $CMRO_2$, which was consistent with the trachea gas samplings shown in Figure 4, and that the obtained OEF values by the approaches of 4PF, 1PF, and BM applied in the present study were not significantly different to that by A–V difference approach as revealed by Bland–Altman analysis.

The simulation study also showed that the most sensitive parameter in $CMRO_2$ was the RW production rate constant, k, followed by Δt. It was therefore suggested that k could be determined with a single blood sampling procedure using the 1PF approach, in which other parameter values were determined and fixed from results from the 4PF approach. It was further showed that k could be obtained from the BM approach as determined from oxygen concentration in the expiration gas. Both 1PF and BM approaches appeared to be robustly useful in $^{15}O_2$ PET for assessing quantitative $CMRO_2$ and CBF in clinical studies.

It is important to note that k varies significantly depending on the physiologic status even in the same species, as seen in Figure 4. According to the simulation study in Figure 1, this variation causes nonnegligible errors in $CMRO_2$, if a constant k is used. Changes in k from 0.1 to 0.6 per min causes errors in $CMRO_2$ of $\pm 30\%$ in anesthetized monkeys. Results from clinical studies, however, showed the variation in k being less. As shown in Table 2, k for clinical patients was 0.129 ± 0.023 per min, and the coefficient of variation was approximately 18%. Previous work by Huang *et al* (1991) also showed similar value with comparable variations, namely 0.131 ± 0.026 per min in six human subjects. These variations caused only $\pm 5\%$ errors in $CMRO_2$, according to the simulation shown in Figure 1. The small variation in k in clinical patients is attributed to the fact that all subjects were studied at a relatively stable condition without physiologic stimulation. However, careful attention is needed if one intends to scan the patients whose whole-body oxygen metabolism is largely changed from the baseline condition. For example, during several pharmacologically stressed (Wessen *et al*, 1997; Kaisti *et al*, 2003), exercise-induced physically stressed, and hyper- or hypothermia (Sakoh and Gjedde, 2003) conditions.

The simulation also showed that size of errors in $CMRO_2$ increased in smaller animals, where the value of k was larger. Recently, $CMRO_2$ as well as CBF have been measured in rats using a small animal PET scanner (Magata *et al*, 2003; Yee *et al*, 2006). Magata *et al* performed multiple blood samplings and plasma separation for multiple blood samples to estimate the RW in their experiment involving rats. The procedures were crucial, but have caused serious alterations of physiologic condition in heart pressure and heart rate due to large amount of blood samples for small animals. Our proposed simplified technique for estimating RW from a single blood sample or from $BMRO_2$, is essential for small animals to be able to maintain the physiologic status. The calculation of $CMRO_2$ also requires whole blood arterial TAC, which can be obtained from arterial blood samplings and could change the physiologic condition. However, such blood sampling could also be avoided by an arterial–venous bypass (Weber *et al*, 2002; Laforest *et al*, 2005), by placing a probe in femoral artery (Pain *et al*, 2004), or by a noninvasive method (Yee *et al*, 2006).

Mintun *et al* (1984) has proposed a simple procedure for RW correction based on a linear interpolation for the bolus $^{15}O_2$ inhalation 60-secs PET scan. As shown in Figure 2, the RW curve is not linear particularly in smaller animals, and a systematic error may be caused or scan duration is limited. Ohta *et al* (1992) and other investigators (Ohta *et al*, 1992; Fujita *et al*, 1999; Vafaee and Gjedde, 2000; Okazawa *et al*, 2001*a*, *b*; Yamauchi *et al*, 2003; Mintun *et al*, 2002), however, have used a technique which does not take into account the RW contribution. Only initial short-period data, namely the 3 mins after the bolus inhalation of $^{15}O_2$, were used in their approach, and thus estimated parameters suffered from statistical uncertainties. The present methodology to estimate RW in the arterial blood allows the prolongation of a PET acquisition period. The technique can also be applicable to the recently proposed sequential administration protocol of $^{15}O_2$ followed by $H_2^{15}O$ to estimate $CMRO_2$ and CBF simultaneously from a single session of a PET scan (Kudomi *et al*, 2005). This protocol, however, required a separation of a RW TAC from the whole blood TAC as showed recently (Kudomi *et al*, 2007).

The k_{BM} determined from the total body oxygen metabolism, namely the BM approach, was significantly greater than k obtained by the 4PF or the 1PF approach, by a factor 2, as shown in Figure 4. The reason is not clear, but partly attributed to the limitation of the simplified model. The body system consists of various organs which have different oxygen metabolism along with different circulation systems and with transit times. It is well known that the apparent rate constant defined with a simplified compartmental model could be underestimated as compared with an average of true rate constants, known as heterogeneity effects (Iida *et al*, 1989; Aston *et al*, 2002). This is, however, not essential.

Simply, linear correction could be applied to convert to the apparent k value as has been performed in this study. $CMRO_2$ values calculated using BM approach for the RW separation, were in good agreement with those determined with the direct measurement of RW as shown in Table 3.

The current method with modeling approach and simplified procedure provided consistent results in terms of time-dependent RW component, and consequently metabolic product of $^{15}O_2$ was separated from arterial whole blood for the $CMRO_2$ assessment in PET examination. The modeling approach to separate metabolite from authentic tracer has been showed previously for 6-[^{18}F]fluoro-L-dopa study (fdopa) (Huang *et al*, 1991). We expect that the modeling approach in conjunction with the simplified method showed in our study could be applied for various kinds of tracers, which require the separation of metabolic product such as fdopa. This approach enables us to assess parametric images for those tracers by eliminating the laborious procedures and by avoiding the amount of blood samplings, particularly for smaller animals.

In conclusion, the present RW model was feasible to reproduce RW TAC from a whole radioactivity concentration curve obtained after $^{15}O_2$ inhalation, and for a wide range of species. The simplified procedure to predict the RW TAC is of use to calculate $CMRO_2$ in smaller animals as well as clinical patients.

Acknowledgements

We acknowledge Mr N Ejima for operating the cyclotron and daily maintenance of CTI ECAT HR. We also gratefully thank Ms Atra Ardekani for her invaluable help on preparing the present paper. We also thank the staff of the Investigative Radiology, Research Institute, National Cardiovascular Center, especially, Dr T Inomata, Dr H Jino, Dr N Kawachi, and Dr T Zeniya for their assistance.

References

Aston JA, Cunningham VJ, Asselin MC, Hammers A, Evans AC, Gunn RN (2002) Positron emission tomography partial volume correction: estimation and algorithms. *J Cereb Blood Flow Metab* 22:1019–34

Eriksson L, Holte S, Bohm Chr, Kesselberg M, Hovander B (1988) Automated blood sampling system for positron emission tomography. *IEEE Trans Nucl Sci* 35:703–7

Eriksson L, Kanno I (1991) Blood sampling devices and measurements. *Med Prog Technol* 17:249–57

Fujita H, Kuwabara H, Reutens DC, Gjedde A (1999) Oxygen consumption of cerebral cortex fails to increase during continued vibrotactile stimulation. *J Cereb Blood Flow Metab* 19:266–71

Hayashi T, Watabe H, Kudomi N, Kim KM, Enmi J, Hayashida K, Iida H (2003) A theoretical model of oxygen delivery and metabolism for physiologic interpretation of quantitative cerebral blood flow and metabolic rate of oxygen. *J Cereb Blood Flow Metab* 23:1314–23

Hirano T, Minematsu K, Hasegawa Y, Tanaka Y, Hayashida K, Yamaguchi T (1994) Acetazolamide reactivity on ^{123}I-IMP single photon emission computed tomography in patients with major cerebral artery occlusive disease: correlation with positron emission tomography parameters. *J Cereb Blood Flow Metab* 14:763–70

Holden JE, Eriksson L, Roland PE, Stone-Elander S, Widen L, Kesselberg M (1988) Direct comparison of single-scan autoradiographic with multiple-scan least-squares fitting approaches to PET $CMRO_2$ estimation. *J Cereb Blood Flow Metab* 8:671–80

Huang SC, Barrio JR, Yu DC, Chen B, Grafton S, Melega WP, Hoffman JM, Satyamurthy N, Mazziotta JC, Phelps ME (1991) Modelling approach for separating blood time-activity curves in positron emission tomographic studies. *Phys Med Biol* 36:749–61

Iida H, Jones T, Miura S (1993) Modeling approach to eliminate the need to separate arterial plasma in oxygen-15 inhalation positron emission tomography. *J Nucl Med* 34:1333–40

Iida H, Kanno I, Miura S, Murakami M, Takahashi K, Uemura K (1989) A determination of the regional brain/blood partition coefficient of water using dynamic positron emission tomography. *J Cereb Blood Flow Metab* 9:874–85

Kaisti KK, Langsjo JW, Aalto S, Oikonen V, Sipila H, Teras M, Hinkka S, Metsahonkala L, Scheinin H (2003) Effects of sevoflurane, propofol, and adjunct nitrous oxide on regional cerebral blood flow, oxygen consumption, and blood volume in humans. *Anesthesiology* 99:603–13

Kudomi N, Choi C, Watabe H, Kim KM, Shidahara M, Ogawa M, Teramoto N, Sakamoto E, Iida H (2003) Development of a GSO detector assembly for a continuous blood sampling system. *IEEE Trans Nucl Sci* 50:70–3

Kudomi N, Hayashi T, Teramoto N, Watabe H, Kawachi N, Ohta Y, Kim KM, Iida H (2005) Rapid quantitative measurement of $CMRO_2$ and CBF by dual administration of ^{15}O-labeled oxygen and water during a single PET scan—a validation study and error analysis in anesthetized monkeys. *J Cereb Blood Flow Metab* 25:1209–24

Kudomi N, Watabe H, Hayashi T, Iida H (2007) Separation of input function for rapid measurement of quantitative $CMRO_2$ and CBF in a single PET scan with a dual tracer administration method. *Phys Med Biol* 52: 1893–908

Laforest R, Sharp TL, Engelbach JA, Fettig NM, Herrero P, Kim J, Lewis JS, Rowland DJ, Tai YC, Welch MJ (2005) Measurement of input functions in rodents: challenges and solutions. *Nucl Med Biol* 32:679–85

Lindstedt L, Schaeffer PJ (2002) Use of allometry in predicting anatomical and physiological parameters of mammals. *Lab Anim* 36:1–19

Magata Y, Temma T, Iida H, Ogawa M, Mukai T, Iida Y, Morimoto T, Konishi J, Saji H (2003) Development of injectable O-15 oxygen and estimation of rat OEF. *J Cereb Blood Flow Metab* 23:671–6

Meyer E, Tyler JL, Thompson CJ, Redies C, Diksic M, Hakim AM (1987) Estimation of cerebral oxygen utilization rate by single-bolus 15O2 inhalation and dynamic positron emission tomography. *J Cereb Blood Flow Metab* 7:403–14

Mintun MA, Raichle ME, Martin WR, Herscovitch P (1984) Brain oxygen utilization measured with O-15 radio-

tracers and positron emission tomography. *J Nucl Med* 25:177–87

Mintun MA, Vlassenko AG, Shulman GL, Snyder AZ (2002) Time-related increase of oxygen utilization in continuously activated human visual cortex. *Neuroimage* 16:531–7

Ohta S, Meyer E, Thompson CJ, Gjedde A (1992) Oxygen consumption of the living human brain measured after a single inhalation of positron emitting oxygen. *J Cereb Blood Flow Metab* 12:179–92

Okazawa H, Yamauchi H, Sugimoto K, Takahashi M, Toyoda H, Kishibe Y, Shio H (2001*a*) Quantitative comparison of the bolus and steady-state methods for measurement of cerebral perfusion and oxygen metabolism: positron emission tomography study using 15O-gas and water. *J Cereb Blood Flow Metab* 21:793–803

Okazawa H, Yamauchi H, Sugimoto K, Toyoda H, Kishibe Y, Takahashi M (2001*b*) Effects of acetazolamide on cerebral blood flow, blood volume, and oxygen metabolism: a positron emission tomography study with healthy volunteers. *J Cereb Blood Flow Metab* 21:1472–9

Pain F, Laniece P, Mastrippolito R, Gervais P, Hantraye P, Besret L (2004) Arterial input function measurement without blood sampling using a beta-microprobe in rats. *J Nucl Med* 45:1577–82

Sakoh M, Gjedde A (2003) Neuroprotection in hypothermia linked to redistribution of oxygen in brain. *Am J Physiol Heart Circ Physiol* 285:H17–25

Shidahara M, Watabe H, Kim KM, Oka H, Sago M, Hayashi T, Miyake Y, Ishida Y, Hayashida K, Nakamura T, Iida H (2002) Evaluation of a commercial PET tomograph-based system for the quantitative assessment of rCBF, rOEF and rCMRO2 by using sequential administration of 15O-labeled compounds. *Ann Nucl Med* 16:317–27

Temma T, Magata Y, Kuge Y, Shimonaka S, Sano K, Katada Y, Kawashima H, Mukai T, Watabe H, Iida H, Saji H (2006) Estimation of oxygen metabolism in a rat model of permanent ischemia using positron emission tomography with injectable ^{15}O-O_2. *J Cereb Blood Flow Metab* 26:1577–83

Vafaee MS, Gjedde A (2000) Model of blood-brain transfer of oxygen explains nonlinear flow-metabolism coupling during stimulation of visual cortex. *J Cereb Blood Flow Metab* 20:747–54

Votaw JR, Shulman SD (1998) Performance evaluation of the Pico-Count flow-through detector for use in cerebral blood flow PET studies. *J Nucl Med* 39:509–15

Weber B, Burger C, Biro P, Buck A (2002) A femoral arteriovenous shunt facilitates arterial whole blood sampling in animals. *Eur J Nucl Med Mol Imaging* 29: 319–23

Wessen A, Widman M, Andersson J, Hartvig P, Valind S, Hetta J, Langstrom B (1997) A positron emission tomography study of cerebral blood flow and oxygen metabolism in healthy male volunteers anaesthetized with eltanolone. *Acta Anaesthesiol Scand* 41:1204–12

Yamauchi H, Okazawa H, Kishibe Y, Sugimoto K, Takahashi M (2003) The effect of acetazolamide on the changes of cerebral blood flow and oxygen metabolism during visual stimulation. *Neuroimage* 20:543–9

Yee SH, Lee K, Jerabek PA, Fox PT (2006) Quantitative measurement of oxygen metabolic rate in the rat brain using microPET imaging of briefly inhaled 15O-labelled oxygen gas. *Nucl Med Commun* 27:573–81

Parametric Renal Blood Flow Imaging Using [^{15}O]H_2O and PET

Nobuyuki Kudomi[1], Niina Koivuviita[2], Kaisa E. Liukko[1], Vesa J. Oikonen[1], Tuula Tolvanen[1], Hidehiro Iida[3], Risto Tertti[2], Kaj Metsärinne[2], Patricia Iozzo[1,4], Pirjo Nuutila[1,2]

[1] *Turku PET Centre, University of Turku, FI 20521, Turku, Finland*

[2] *Department of Medicine, University of Turku, Turku, Finland*

3 Department of Investigative Radiology, Advanced Medical-Engineering Center, National Cardiovascular Center-Research Institute, 5-7-1, Fujishirodai, Suita, Osaka, 565-8565, Japan

[4] *Institute of Clinical Physiology, National Research Council, 56100 Pisa, Italy*

Running title: RBF imaging by PET

Corresponding author

Nobuyuki Kudomi, PhD

Turku PET Centre, University of Turku

PO Box 52, FIN-20521, Turku, Finland

Phone: +358-2-313-2772

Fax: +358-2-231-8191

E-mail: nobuyuki.kudomi@tyks.fi

Abstract

The quantitative assessment of renal blood flow (RBF) would allow the understanding of the physiological basis of kidney function and the evaluation of pathophysiological events leading to vascular damage, such as renal arterial stenosis and chronic allograft nephropathy. The RBF may be quantified using PET with $H_2{}^{15}O$, although RBF studies that have been performed without theoretical evaluation, have assumed the partition coefficient of water (p ml/g) as uniform for whole region of renal tissue, and/or radioactivity from vascular space (V_A ml/ml) as negligible. The aim of this study is to develop a method to calculate parametric images of RBF (K_1, k_2) as well as V_A without fixing the p by the basis function method (BFM). The feasibility was tested in healthy subjects. A simulation study was performed to evaluate error sensitivities for possible error sources. Experimental study showed that the quantitative accuracy in the present method was consistent to nonlinear least-squares fitting, i.e., $K_{1,BFM}=0.93K_{1,NLF}$ -0.11 ml/min/g ($r=0.80$, $P<0.001$), $k_{2,BFM}=0.96k_{2,NLF}$–0.13 ml/min/g ($r=0.77$, $P<0.001$) and $V_{A,BFM}=0.92V_{A,NLF}$-0.00 ml/ml ($r=0.97$, $P<0.001$). Akaike information Criterion values from the present fitting are the smallest for all subjects except two. The quality of parametric images obtained was acceptable. The simulation study suggested that delay and dispersion time constants should be estimated within 2-sec accuracy. V_A and p cannot be neglected or fixed, and reliable measurement of even relative RBF values requires that V_A is fitted. We conclude that this study shows the feasibility of measurement of RBF using PET with $H_2{}^{15}O$.

Key words: Positron emission tomography, renal blood flow, compartment model, parametric image

Introduction

The quantitative assessment of renal blood flow (RBF) may help to understand the pathophysiological basis of kidney function and to evaluate pathophysiological events leading to vascular damage, such as renal arterial stenosis and chronic allograft nephropathy. The quantitative estimation of RBF by use of $H_2{}^{15}O$ and dynamic PET has been developed and demonstrated by Nitzsche et al [1]. The kinetic model of $H_2{}^{15}O$ has been based on the assumptions that all activity is extracted by the parenchyma, extraction is very rapid, and tubular transport has not started or is insignificant at a level that does not influence the calculation of renal blood flow [1-5]. From this assumption, region of interest (ROI) based estimation of RBF has been performed by the $H_2{}^{15}O$ dynamic PET approach [1, 3, 4]. Also, calculation of parametric RBF images has been performed [5]. However, the quantitative computation of RBF, so far, has assumed that the blood/tissue partition coefficient of water (p ml/g) was uniform for the whole region of renal tissue [3, 4], and/or that the contribution of radioactivity from vascular space was negligible [5-7]. The influence of quantitative accuracy from those assumptions is unknown.

The previous studies demonstrated to compute RBF from uptake rate (K_1 ml/min/g) [1-7]. Some studies also simultaneously compute p [6, 7], and the obtained apparent p value was ranged between 0.52 and 0.78 ml/g. From published values of water content for tissue as 76 % and for blood as 81 % [8], the p value can be physiologically determined as: p_{phys}=0.94 ml/g [9]. The extremely smaller apparent p value might be due to tissue mixture (or partial volume effect) [10, 11] because of composite structure of kidney. The effects of tissue mixture affect mostly K_1 and not clearance rate (k_2 min^{-1}). Therefore clearance rate of $H_2{}^{15}O$ (k_2 min^{-1}) multiplied by p_{phys} could be applied for the blood flow rather than K_1 ml/min/g [11], when affect of tissue mixture is not negligible, although it is unknown how the glomerular

filtration rate (GFR) additionally contribute to k_2. Thus, the influence of GFR on k_2 should be evaluated and corrected in the computation of RBF

The aim of this study was to develop a method to simultaneously calculate parametric images of K_1 and k_2 as well as the arterial blood volume (V_A ml/ml). The feasibility, in terms of quantitative accuracy and image quality on calculated images, were experimentally tested in healthy subjects. GFR was measured for each subject to investigate how much it contributes to the clearance rate (k_2 min^{-1}). A simulation study was also performed to evaluate error sensitivities for possible error sources.

Materials and methods

Theory

The present formula was characterized by simultaneously estimating multiple parameters of uptake rate constant (K_1 ml/min/g) and clearance rate constant (k_2 ml/g) as well as activity concentration in arterial vascular space (V_A ml/ml). The kinetic model for $H_2{}^{15}O$ was based on the single tissue compartment model as;

$$Ci(t) = (1 - V_A) \cdot K_1 \cdot A_w(t) \otimes e^{-k2 \cdot t} + V_A \cdot A_w(t) \qquad (1)$$

where $Ci(t)$ (Bq/mL) is radioactivity concentration in a voxel of PET image, $A_w(t)$ (Bq/mL) is the arterial input function, $\otimes$ indicates the convolution integral..

In the present computation, we have applied a basis function method (BFM), which was introduced by Koeppe et al [12] to compute cerebral blood flow parametric image as well as the clearance rate constant simultaneously. Gunn et al [13] applied this method to parametric imaging of both binding potential and the delivery of the ligand relative to the reference region. The computation method has also been applied to myocardial blood flow studies to compute the uptake, clearance rates and blood volume [14, 15]. The BFM procedure for the present RBF computation is illustrated in Figure 1. The BFM method

enables to compute parametric images by using linear least squares together with a discrete range of basis functions as the parameter value for k_2 incorporating the nonlinearity and covering the expected physiological range. The corresponding basis functions formed as;

$$F(k_2,t) = A_w(t) \otimes e^{-k2 \cdot t} \tag{2}$$

For the physiologically reasonable range of k_2, i.e., $0 < k_2 < 15.0$ ml/min/g, 1500 discrete values for k_2 were found to be sufficient. Then Eq. (1) can then be transformed for each basis function into a linear equation as;

$$\begin{aligned} &Ci(t) = \Theta \cdot F(k_2,t) + \Psi \cdot A_w(t) \\ &\Theta = (1 - V_A) \cdot K_1 \\ &\Psi = V_A \end{aligned} \tag{3}$$

Hence for fixed values of k_2, the remaining two parameters Θ and Ψ can be estimated using given basis function by standard linear least squares, and obtained as: Θ_{k2} and Ψ_{k2}. The k_2 for which the residual sum of square;

$$s(k_2)^2 = \sum_t (Ci(t) - \Theta_{k2} \cdot F(k_2,t) - \Psi_{k2} \cdot A_w(t))^2 \tag{4}$$

is minimized is determined by a direct search and associated parameter values for this solution (K_1, k_2, V_A) are obtained.

Subjects

Six healthy human subjects (the demographics are shown in Table 1) were studied under the basal as well as under stimulation (after enalapril infusion) conditions. All subjects were non-smoking and none of them was taking any medication. All subjects gave written informed consent. The study was approved by the Ethical Committee of the Hospital District of South-Western Finland, and was conducted with the Declaration of Helsinki as revised in 1966.

PET Experiments

PET acquisition was carried out in 2D mode using the GE Advance PET scanner (GE Medical Systems, Milwaukee, Wis). After 300-sec transmission scan, two scans were undertaken with $H_2{}^{15}O$ (1.0 to 1.5 GBq) injection from cephalica vein in the right forearm. First scan was under resting conditions and the other was in stimulated conditions, namely, 20 min after 0.5 mg enalapril infusion. Scan protocol consisted of 20 frames with total of 240 sec (15×4 sec, and 5×10 sec).

During PET scanning, blood was withdrawn continuously through a catheter inserted in the left radial artery by using a peristaltic pump (Scanditronix, Uppsala, Sweden). Radioactivity concentrations in blood were measured with a BGO coincidence monitor system. The detectors had been cross-calibrated to the PET scanner *via* ion chamber [16].

Also, glomerular filtering ratio (GFR) was measured for each subject [17]. To obtain the PET equivalent flow ratio for GFR, kidney weight of 300 g and cortex ratio of 70 % were assumed [8].

Data Processing

Dynamic sinogram data were corrected for dead time in each frame in addition to detector normalization. Tomographic images were reconstructed from corrected sinogram data by the OSEM method using a Hann filter with a cut-off frequency of 4.6 mm. Attenuation correction was applied with transmission data. A reconstructed image consisted 128×128×35 matrix size with a pixel size of 4.3 mm × 4.3 mm and 4.2 mm with 20 frames.

Measured arterial blood time activity curves (TAC) were calibrated to the PET scanner and corrected for the dispersion (τ=5 and 2.5 sec for intrinsic and extrinsic, respectively) [18] and delay [19]. The corrected blood TAC was used as the input function.

A set of K_1, k_2 and V_A images were generated according to the BFM formula described above, using a set of dynamic reconstructed image and input function. Computations were programmed in C environment (gcc 3.2) on Sun workstation (Solaris 10 Sun Fire 280R) with 4 GB of memory and two Sparcv9, 900-MHz CPUs.

Data Analysis

A template of ROI was drawn on the whole region of each kidney on an image, which was obtained by summing whole frames of reconstructed dynamic image (average ROI sizes for the all subjects was 153 ± 43 cm^3). Also, a ROI was drawn on a region of high tracer accumulation on the summed image as an assumed cortical region. Functional values of K_1, k_2 and V_A were extracted from both of ROIs, i.e., for whole and cortical regions, respectively. Data were shown individually or as mean±SD. The Student's paired *t*-test was used for comparisons between the physiological states and $P<0.05$ was considered as significant.

The ROI for whole region was divided plane-by-plane into sub-regions of 10 pixels each. The sub-regions were created by extracting pixels firstly from horizontal then vertical directions inside the whole ROI in each slice. Each sub-region consisted of a single area with the same number of pixels. Functional values of K_1, k_2 and V_A were extracted from each sub-region. Also, tissue TACs were obtained in each sub-region from corresponding dynamic images. The three parameters of K_1, k_2 and V_A were estimated by using the Equation (1) and input function fitting to the tissue TACs by means of the nonlinear least-squares fitting method (NLF) (Gauss-Newton method). Then, functional values of K_1, k_2 and V_A from corresponding sub-regions were compared between the methods. The regression analysis was performed.

Model relevancy among introducing p and/or V_A in the computation was tested using the Akaike Information Criterion (AIC) [20]. The most appropriate model provides the

smallest AIC. The tissue TACs from above sub-regions were fitted and AICs were computed for models with three parameters of K_1, k_2 and V_A, fixing $p(=K_1/k_2)$ at 0.35 ml/g (mean value obtained in the present subjects), fixing V_A at 0 ml/ml, and fixing V_A at 0.15 ml/ml (mean value obtained in the present subjects).

Error Analyses in Simulation

Error propagation from error in input function for the present BFM formula was analyzed for two factors: delay and dispersion in arterial TAC. It is known that the measured arterial TAC is delayed and more dispersed relative to the true input TAC in the kidney because of the time and tube transit of blood through the peripheral artery and catheter tube before reaching the detector [18, 19]. Calculation of RBF, so far, employed a fixed partition coefficient: $p(=K_1/k_2)$ ml/g and/or assumed the blood volume: V_A ml/ml as negligible, throughout the whole renal region and did not estimate it regionally. BFM formulae with fixed value of p (BFM-pfix), and blood volume V_A (BFM-vfix) in addition to the present BFM formula and error in those formulae were analyzed.

A typical arterial input function obtained from the present PET study was used in the present simulation as the true input function. Applying this input function to the water kinetic model in Eq. (1), a tissue TAC was created assuming values of normal kidney tissue (K_1 = 2.0 ml/min/g, V_A=0.14 ml/g [5], and p = 0.4 ml/g (corresponding to the estimated mean in cortical regions for all subjects in this study)).

Time in input function was shifted from -4 to 4 sec to simulate the error sensitivity due to error in delay time, where a positive error represents an overcorrection of delay time. Input function was convoluted or deconvoluted with a simple exponential [18] by shifting the time constant from -4 to 4 sec to simulate the error sensitivity due to error in dispersion correction, where a negative error represents undercorrection, as described previously [18, 21].

Values of K_1 and k_2 were calculated using simulated input functions and above assumed tissue TACs based on the BFM formula. Errors in these calculated K_1 and k_2 values were presented as percentage differences from the assumed values. Then, the value of p was varied from 0.3 to 0.5 ml/g and tissue TAC was generated as above for simulating the error from the value of p in BFM-pfix formula. Also, V_A value was varied from 0.0 to 0.4 ml/ml and tissue TAC was generated for simulating the error from V_A in BFM:vfix formula. Then, K_1 and k_2 were calculated using the true input function and the created tissue TACs, assuming p = 0.4 ml/g and V_A =0.0 ml/ml in BFM-pfix and BFM-vfix formulae, respectively. Error in K_1 and k_2 values due to fixing p was presented as percent difference of K_1 and k_2 as a function of p. Error in K_1 and k_2 values due to neglecting V_A was presented as percent difference of K_1 and k_2 as a function of V_A. Also, K_1 and k_2 were computed with fixing V_A as 0.14 ml/ml in BFM-vfix formula from the set of the above created tissue TAC, in which K_1 and p were fixed to 2.0 ml/min/g and 0.4 ml/g, respectively, and V_A was varied. Percent difference of K_1 and k_2 between two conditions, i.e., the initial (K_1 = 2.0 ml/min/g and V_A = 0.14 ml/ml) and changed conditions (presented as ΔK_1 and Δk_2, respectively) was presented as a function of the percent difference of assumed V_A from 0.14 ml/ml (ΔV), to investigate the extent to watch the change of K_1 and k_2 was estimated when K_1 and k_2 was computed in BFM-vfix formula.

Results

Experiments

The relationships of the regional ROI values of K_1, k_2 and V_A between NLF and BFM are shown in Fig 2. The regression lines obtained were $K_{1,BFM}$ = 0.93 $K_{1,NLF}$ -0.11 ml/min/g (r = 0.80, $P<0.001$), $k_{2,BFM}$ = 0.96 $k_{2,NLF}$ – 0.13 ml/min/g (r = 0.77, $P<0.001$) and $V_{A,BFM}$ = 0.92 $V_{A,NLF}$ -0.00 ml/ml (r = 0.97, $P<0.001$), for K_1, k_2 and V_A, respectively, where subscripts at the

parameter show the methods to calculate parametric values, and showed that the slope were not significantly different from the unity.

The fitted curve by the present model with estimating K_1, k_2 and V_A fitted well than the other two models with fixing $p(=K_1/k_2)$ or V_A. One example of fitted curves is shown in Fig 3. Also, the Akaike Information Criterion (AIC) values from three parameters fitting are the smallest for all subjects except two values for two parameter fittings with fixing V_A in patient 2 and fixing p in patient 3, although some of AIC values are similar (Table 2). These results show the present method with three parameters fitting is feasible to compute RBF.

Quantitative values of K_1, $k_2 \cdot p_{phys}$ and V_A were obtained for whole and cortical regions (Table 3). The K_1 values were smaller than $k_2 \cdot p_{phys}$ values and the ratio between them was ranged from 0.35 to 0.45, suggesting K_1 values were underestimated than RBF due to the partial volume effect. Both K_1 and $k_2 \cdot p_{phys}$ were not significantly different between the resting and stimulating conditions after enalapril administration for whole and cortical regions, respectively, although the value of V_A became higher in stimulating than basal conditions. The GFR value obtained was 78 ± 4 ml/min, corresponding to the clearance rate of 0.37 ± 0.02 ml/min/g and to 9.6 % to the k_2 obtained for cortical region in normal condition.

K_1 and $k_2 \cdot p_{phys}$ images generated by the present method are representatively shown in Fig. 4. The image is shown in acceptable quality. The K_1 and $k_2 \cdot p_{phys}$ value is from 1.5 to 2.0 ml/min/g and 3.0 to 5.0 around cortical region, respectively, and some parts show higher value than those, respectively. The average time required to compute the parametric images was 2 min and 23 sec.

Error Analyses

The size of error introduced in both K_1 and k_2 was less than 20% for an error in the estimation of delay and in the dispersion time constant up to 2 sec (Fig. 5). The error sensitivity in K_1 and

k_2 was 40 % when the partition coefficient was 0.35 (Fig 6). The magnitude of error was remarkably enhanced when the blood volume was ignored (Fig 7a), and if the size of arterial blood volume changed to be 25 % larger, K_1 and k_2 was overestimated by 20 % (Fig 7a).

Discussion

We have presented an approach to generate quantitative K_1, k_2 and V_A images using $H_2{}^{15}O$ and PET applying BFM computation method. This article described the validity of this approach in healthy human subjects under resting and stimulating conditions. The rate constant values of K_1 and $k_2 \cdot p_{phys}$ obtained from parametric images were consistent against NFL and quality of K_1 and $k_2 \cdot p_{phys}$ images obtained was acceptable. The smaller K_1 against $k_2 \bullet p_{phys}$ values suggested that K_1 value was underestimated than absolute RBF value due to partial volume effect. The simulation showed that the delay time and dispersion time constant should be estimated within 2 sec accuracy, and V_A and p cannot be ignored/fixed to estimate the rate constants of K_1 and/or k_2. Also V_A cannot be ignored, even when only relative rate constant values are needed. These findings suggest that the present k_2 obtained BFM technique provides RBF image with reasonable accuracy and quality.

The present study experimentally computed the rate constants of K_1 and k_2, and those ratio obtained was ranged from 0.35 to 0.45 ml/g, which corresponds to the apparent kidney-blood partition coefficient. The extremely smaller apparent p value might be due to partial volume effect, as has been demonstrated in the previous brain and cardiac study [10, 11], because of composite structure in kidney, spatial resolution of reconstructed image and breathing movement of patient during the scan. When the rate constant of K_1 is underestimated due to partial volume effect, $k_2 \bullet p_{phys}$ could be applied for the RBF rather than K_1. The present study showed the smaller contribution of GFR as only 10 % to the clearance rate, $k_2 \bullet p_{phys}$ is more appropriate for RBF assessment, although further study is required how